Clinical Imaging 50 (2018) 147–156

Contents lists available at ScienceDirect

Clinical Imaging

journal homepage: www.elsevier.com/locate/clinimag

Pediatric Radiology

Free-breathing 320-row computed tomographic angiography with low-tube voltage and hybrid iterative reconstruction in infants with complex congenital heart disease

Yuzo Yamasaki[a,*], Satoshi Kawanami[b], Takeshi Kamitani[b], Koji Sagiyama[b], Seitaro Shin[b], Takuya Hino[b], Kenichiro Yamamura[c], Hidetake Yabuuchi[d], Michinobu Nagao[e], Hiroshi Honda[b]

[a] Department of Molecular Imaging & Diagnosis, Graduate School of Medical Sciences, Kyushu University, Japan
[b] Department of Clinical Radiology, Graduate School of Medical Sciences, Kyushu University, Japan
[c] Department of Pediatrics, Graduate School of Medical Sciences, Kyushu University, Japan
[d] Department of Health Sciences, Graduate School of Medical Sciences, Kyushu University, Japan
[e] Department of Diagnostic Imaging and Nuclear Medicine, Tokyo Women's Medical University, Japan

ARTICLE INFO

Keywords:
Congenital heart disease
Infant
Iterative reconstruction
Low-tube voltage
Multi-detector computed tomography

ABSTRACT

We explored the clinical value of low-tube voltage prospective second-generation ECG-triggered 320-row CT angiography in infants with complex CHD (37 male, 23 female, aged 0–2 years). The diagnostic accuracy of 320-row CT in complex CHD was 99.4% for intracardiac cardiovascular malformations, 99.8% for extracardiac cardiovascular malformations, and 100% for other malformations. The average subjective overall image quality score for cardiac structures was 3.7 ± 0.5 points. Second-generation 320-row CT angiography with low-tube voltage and prospective ECG-triggered volume target scanning allows accurate diagnosis of cardiovascular anomalies in infants with complex CHD.

1. Introduction

Conventional cardiac angiography (CCA) is a recognized gold standard method for evaluating complex congenital heart disease (CHD) in infants. However, catheterization of an infant or young child, especially one with complex CHD, is rather difficult because of the patient's small size and inability to cooperate. Moreover, CCA is an invasive procedure with an approximately 1% intraoperative mortality rate [1], and there is also the potential for high exposure to radiation [2].

Because of these risks, non-invasive examination methods have replaced invasive angiography for the detection of complex CHD in infants. Transthoracic echocardiography is often used to diagnose CHD, but the limits of the acoustic window, poor spatial resolution, and the subjectivity of the operator's judgments are major drawbacks to this procedure [3]. Moreover, transthoracic assessment of the inner structures of the body that are far from the chest wall, such as the pulmonary vein, aortic arch, and descending aorta, is sometimes problematic.

In recent years, cardiac magnetic resonance imaging (MRI) has developed rapidly as a diagnostic tool, and can be used for evaluation of both cardiac anatomy and function. However, this type of examination requires specialized hardware and experience, which is not universally available [4]. Further, neonatal cardiac MRI involves relatively long imaging times, usually requires general anesthesia with intubation for suspended respiration, and decreased signal-to-noise ratios and high baseline heart rates pose technical challenges in the smallest patients. MRI with anesthesia has been shown to be generally safe, but the highest risks of adverse anesthetic events with MRI are in hospitalized patients and in patients younger than 1 year of age. The relative risk of an adverse event during a cardiac MRI if performed with anesthesia is 3.9 [5–7]. In addition, repeated or prolonged use of general anesthetics or sedative drugs during early childhood may be associated with negative effects on the developing brain [8–11]. These effects include an increased risk of developing learning difficulties such as impaired language and communication skills [10] as well as behavioral or developmental problems [11].

Recently, the spatial and temporal resolution of multi-slice computed tomography (CT) has been greatly improved, and this method has been increasingly used in the diagnosis of CHD in infants and young children. The faster scan time, and the better image quality can be

Abbreviations: CCA, conventional cardiac angiography; CHD, congenital heart disease; CT, computed tomography; ECG, electrocardiogram; MRI, magnetic resonance imaging

* Corresponding author at: Department of Molecular Imaging & Diagnosis, Graduate School of Medical Sciences, Kyushu University, 3-1-1 Maidashi, Higashi-ku, Fukuoka 812-8582, Japan.
E-mail address: yyama@radiol.med.kyushu-u.ac.jp (Y. Yamasaki).

https://doi.org/10.1016/j.clinimag.2018.02.008
Received 17 November 2017; Received in revised form 2 February 2018; Accepted 7 February 2018

useful for infants who cannot hold their breath. A slice obtained by second-generation 320-row CT prospective electrocardiogram (ECG)-gating takes only 0.275 s to acquire because of its more rapid gantry rotation and 16 cm z-axis coverage in almost all cases of complex CHD. The temporal resolution of this latest CT technique has a volume scanning mode, which can reach 137.5 ms and can achieve 180°/360° without moving. This provides the data of all organs and avoids the migration data error caused by the placement movement of patients from spiral scanning, the time interval difference of image composition, and the unnecessary scan dose caused by repetitive scanning [12]. In clinical practice, a shorter scan time is needed for sedated children who cannot hold their breath. This imaging method is preferred for cardiac CT angiography in patients with a high heart rate, especially infants and children, and may be the best way of evaluating infants with complex CHD. Further, the combination of low-tube voltage and hybrid iterative reconstruction can lower the radiation dose exposure without impairing image quality [13]. However, there are few reports on the use of 320-row CT and there is very little information on its use for diagnostic purposes in infants with complex CHD [12]. To our knowledge, there have been no studies demonstrating the clinical utility of prospective ECG-triggered second-generation 320-row CT angiography, with the combination of low-tube voltage and hybrid iterative reconstruction in infants. Further, there have been no studies of the effect of body size (which can vary widely in the course of days in infants) on the visibility of cardiac structures in this age group.

The aim of this study was to explore the clinical value and detectability of low-dose prospective ECG-triggered 320-row CT angiography based on age and body size in infants with complex CHD.

2. Methods

The study protocol was approved by the institutional review boards of the participating institutions. The need for written informed consent was waived in view of the retrospective nature of the research.

The study included 60 consecutive infants with complex CHD (37 male, 23 female, aged 0–2 years) who underwent examination by 320-row CT angiography with low-dose prospective ECG-triggered volume target scanning between August 2015 and January 2017. At our institution, CT angiography is part of the cardiovascular evaluation in patients with complex CHD and is performed as clinically indicated. Complex CHD is defined as CHD with more than one distinct cardiovascular anomaly, and all anomalies were confirmed by surgical and/or CCA findings.

2.1. 320-Row CT scan protocol

The examinations were performed using a second-generation 320-detector row CT scanner (Aquilion ONE Vision; Toshiba Medical Systems, Nasu, Japan), which has a detector width of 160 mm and 320 detector rows. The CT gantry has a minimum rotation time of 275 ms. All tests using 320-row CT angiography with prospective ECG-triggered mode were performed while the children were breathing freely. A chloral hydrate enema was used for sedation during scanning and the dose was calculated based on each child's body weight and clinical need. Iodinated contrast medium (Iopamiron, 300 mg I/mL, Bayer, Tokyo, Japan) was injected via a peripheral vein using a double-head power injector (Nemoto Kyorindo Co. Ltd., Tokyo, Japan) with a volume of 2.0 mL/kg body weight followed by a saline chaser of 0.67 mL/kg body weight. The injection rate was calculated as the total injected volume divided by 80 s, and the data acquisition was performed at 80 s. For example, a 6-kg baby would be injected with 12 mL of contrast medium and 4 mL of saline at a flow rate of 0.2 mL per second. The scan volume was set to the whole chest, extending from the supraclavicular level superiorly to just below the diaphragm inferiorly. In cases of suspected heterotaxy or anomalous inferior vena cava drainage, the scan volume was extended to the infrarenal region. The patients were imaged using a prospective triggered target CT angiographic volume scan with a rotation time of 0.275 s and a tube voltage of 80 kVp. The center for the data acquisition phase window in this study was set to 45% of the R–R interval. The scan range depended on the patient's size and heart rate as well as the area to be evaluated, which varied from 10 cm to 16 cm, and the tube current was set by automatic exposure control (noise level, standard deviation 20; thickness, 0.5 mm). The effective dose was derived from the dose-length product and conversion coefficients for the chest, taking into account the patient's age [14,15].

2.2. Image post-processing and analysis

Full volumes were reconstructed in 0.5 mm-thickness slices. In addition to the CT axial images, multiplanar reconstruction, volume rendering reconstruction, and maximum intensity projection images can also be used to display heart malformations.

The CT images were interpreted without knowledge of the results of surgery, CCA, or transthoracic echocardiography. CT angiographic images were presented in random order. Using surgical and/or CCA findings as the reference standard, the diagnostic accuracy was evaluated based on patient age. The overall image quality was evaluated semi-quantitatively by two board-certified radiologists (SK and KS) with over 5 years of diagnostic experience in cardiac radiology. If a reviewer was the original primary reader for the case, they would only be able to evaluate it again after > 3 months from the initial clinical reading. The evaluation criteria were based on a five-point rubric (5, excellent anatomical clarity and image quality; 4, good anatomical clarity, all structures are clearly interpretable; 3, fair anatomical clarity, the anatomical relationships can be defined with relative confidence; 2, poor image quality or anatomical detail, incomplete demonstration of anatomical structures; 1, no useful information obtained) [15].

In the event of disagreement in scoring between the two observers, the mean of the two results was used for the score. Examinations graded over 3 were considered sufficient for complete diagnosis.

2.3. Evaluation of radiation dose

The radiation exposure parameters, comprising imaging range, dose-length product, and volume CT dose index [16], were recorded for each infant who underwent CT angiographic examination. The cardiac CT angiographic effective dose was calculated from the dose-length product multiplied by the conversion factor [17]. The size of the CT dose index phantom was 16 cm. The specific dose-length product conversion coefficients for infants vary according to age as follows: younger than 4 months, 0.039 mSv/[mGy·cm]; age 4 months to 1 year, 0.026 mSv/[mGy·cm]; and age 1 year to 6 years, mSv/[mGy·cm] [14,15].

2.4. Statistical analysis

The measurement data are expressed as the means ± standard deviation. The results of surgery or CCA were regarded as the reference standard when calculating the diagnostic accuracy of 320-row CT. The diagnostic consistency of the two readers for subjective image quality scoring was processed using the kappa statistic as follows: 0, no agreement; 0.01–0.20, poor agreement; 0.21–0.400, fair agreement; 0.41–0.600, moderate agreement; 0.61–0.80, substantial agreement; and 0.81–0.99, almost perfect agreement. A P-value < 0.05 was considered to be statistically significant.

3. Results

Patient characteristics are shown according to age in Table 1. There were 105 intracardiac cardiovascular malformations, 76 extracardiac

Table 1
Patients characteristics.

	N	BW (g)	HR (/min)	Radiation exposure (mSv)
~1 month	11	2718	140	1.19
1–3 months	17	3395	138	1.35
4–6 months	8	3903	125	1.14
7 months–1 year	10	5991	120	1.38
1–2 years	14	8001	120	1.23

N, number of patients; BW, body weight; HR, heart rate.

cardiovascular malformations, and 15 other malformations (Table 2). The diagnostic accuracy of 320-row CT in complex CHD was 99.4% for intracardiac cardiovascular malformations (Table 3), 99.8% for extracardiac cardiovascular malformations (Table 4), and 100% for other malformations (Table 5). Some typical cases are shown in Figs. 1–3.

Four intracardiac cardiovascular malformations were misdiagnosed by 320-row CT, including one case of an atrial septal defect, two cases of a ventricular septal defect, and one case of pulmonary stenosis.

Two extracardiac cardiovascular malformations evaded detection on 320-row CT, including one case of partial anomalous pulmonary venous return and one of a single coronary artery. Anomalous return of the right upper pulmonary vein evaded detection in a male infant at the age of 1 month and a body weight of 2684 g, but was diagnosed when the infant reached the age of 16 months and had a body weight of 8390 g (Fig. 4).

All intracardiac cardiovascular malformations were diagnosed correctly after the age of 4 months or when the infants weighed > 5 kg, and all extracardiac cardiovascular malformations were diagnosed correctly after the age of 7 months or when the infants weighed 7.5 kg (Tables 6 and 7).

3.1. Subjective assessment of image quality

The image quality score for each structure is shown in Table 8. In addition to the overall image quality scores, the mean image quality scores for all structures were 3 points or more, regardless of patient age. The average subjective overall image quality score for second-generation 320-row CT angiography, with prospective ECG-triggered volume target scanning in the cardiac structures, was 3.7 ± 0.5 (range 3–5) points. The consistency for all image quality scores between the two readers was moderate, with a k value of 0.56.

3.2. Evaluation of radiation dose

The mean dose-length product was 45.71 ± 18.75 mGy·cm and the mean effective radiation dose was 1.27 ± 0.39 mSv. There were no statistically significant age-related differences in these parameters.

4. Discussion

This 320-row cardiac CT study on detectability of CHD in infants demonstrated the following: 1) second-generation 320-row CT angiography with prospective ECG-triggered volume target scanning and hybrid iterative reconstruction has high diagnostic accuracy in the

Table 2
Diagnoses of deformities in a cohort of 60 infants.

	~1 month	1–3 months	4–6 months	6 months–1 year	1–2 years	Total
Intracardiac malformations						
Atrial septal defect/patent foramen ovale	3	7	6	4	3	23
Ventricular septal defect	4	8	5	6	6	29
Atrioventricular septal defect	1	2	1	3	1	8
Atrioventricular discordance	1	1			1	3
Ventriculoarterial discordance	1	1			1	3
Single right ventricle	1	1	2	2		6
Overriding aorta	1	4			2	7
Pulmonary stenosis/atresia	3	5	2	2	6	18
Aortic stenosis/atresia		1	1			2
Tricuspid stenosis/atresia				1		1
Mitral stenosis/atresia		2	2	1		5
Total	15	32	19	19	20	105
Extracardiac malformations						
Double outlet right ventricle		2	2	2	1	7
Truncus arteriosus communis	1					1
Pulmonary artery stenosis		1		2	3	6
Dilated pulmonary artery	1	1				2
Anomalous origin of pulmonary artery	1	1				2
Patent ductus arteriosus	5	6	3	2	2	18
Anomalous pulmonary venous return	1	2			1	4
Pulmonary vein stenosis		2	1	1	2	6
Vena cava stenosis				1	2	3
Coarctation of the aorta	3	3	4	1		11
Interrupted aortic arch	1					1
Major aortopulmonary collateral artery					1	1
Right aortic arch	2	1				3
Double superior vena cava (SVC)/left SVC	3	1	2		1	7
Coronary artery anomaly	1		3	4	1	9
Total	19	20	15	13	14	81
Other malformations						
Asplenia	3					3
Thymic hypoplasia	3	1	3	1		8
Tracheobronchial anomalies	2	2				4
Total	8	3	3	1		15

Table 3
Findings of intracardiac malformations at prospective ECG-triggering 320-row MDCT angiography in reference to surgical findings and/or conventional cardiac angiography.

	~1 month				1–3 months				4–6 months				6 months–1 year				1–2 years				Total			
Intracardiac malformations	TP	TN	FP	FN	TP	TN	FP	FN	TP	TN	FP	FN	TP	TN	FP	FN	TP	TN	FP	FN	TP	TN	FP	FN
Atrial septal defect/patent foramen ovale	3	8	0	0	6	10	0	1	6	2	0	0	4	6	0	0	3	11	0	0	22	37	0	1
Ventricular septal defect	4	6	1	0	7	9	0	1	5	3	0	0	6	4	0	0	6	8	0	0	28	30	1	1
Atrioventricular defect	1	10	0	0	2	15	0	0	1	7	0	0	3	7	0	0	1	13	0	0	8	52	0	0
Atrioventricular discordance	1	10	0	0	1	16	0	0	0	8	0	0	0	10	0	0	1	13	0	0	3	57	0	0
Ventriculoarterial discordance	1	10	0	0	1	16	0	0	0	8	0	0	0	10	0	0	1	13	0	0	3	57	0	0
Single right ventricle	1	10	0	0	1	16	0	0	2	6	0	0	2	8	0	0	0	14	0	0	6	54	0	0
Overriding aorta	1	10	0	0	4	13	0	0	0	8	0	0	0	10	0	0	2	12	0	0	7	53	0	0
Pulmonary stenosis/atresia	3	7	1	0	5	12	0	0	2	6	0	0	2	8	0	0	6	8	0	0	18	41	1	0
Aortic stenosis/atresia	0	11	0	0	1	16	0	0	1	7	0	0	0	10	0	0	0	14	0	0	2	58	0	0
Tricuspid stenosis/atresia	0	11	0	0	0	17	0	0	0	8	0	0	1	9	0	0	0	14	0	0	1	59	0	0
Mitral stenosis/atresia	0	11	0	0	2	15	0	0	2	6	0	0	1	9	0	0	0	14	0	0	5	55	0	0
Total	15	104	2	0	30	155	0	2	19	69	0	0	19	91	0	0	20	134	0	0	103	553	2	2

Accuracy: 99.4%.
TP, true positive; TN, true negative; FP, false positive; FN, false negative.

Table 4
Findings of extracardiac malformations at prospective ECG-triggering 320-row MDCT angiography in reference to surgical findings and/or conventional cardiac angiography.

	~1 month				1–3 months				4–6 months				6 months–1 year				1–2 years				Total			
Extracardiac malformations	TP	TN	FP	FN	TP	TN	FP	FN	TP	TN	FP	FN	TP	TN	FP	FN	TP	TN	FP	FN	TP	TN	FP	FN
Double outlet right ventricle	0	11	0	0	2	15	0	0	2	6	0	0	2	8	0	0	1	13	0	0	7	53	0	0
Truncus arteriosus communis	1	10	0	0	0	17	0	0	0	8	0	0	0	10	0	0	0	14	0	0	1	59	0	0
Pulmonary artery stenosis	0	11	0	0	1	16	0	0	0	8	0	0	2	8	0	0	3	11	0	0	6	54	0	0
Dilated pulmonary artery	1	10	0	0	1	16	0	0	0	8	0	0	0	10	0	0	0	14	0	0	2	58	0	0
Anomalous origin of pulmonary artery	1	10	0	0	1	16	0	0	0	8	0	0	0	10	0	0	0	14	0	0	2	58	0	0
Patent ductus arteriosus	5	6	0	0	6	11	0	0	3	5	0	0	2	8	0	0	2	12	0	0	18	42	0	0
Anomalous pulmonary venous return	1	10	0	0	1	15	0	1	0	8	0	0	0	10	0	0	1	13	0	0	3	56	0	1
Pulmonary vein stenosis	0	11	0	0	2	15	0	0	1	7	0	0	1	9	0	0	2	12	0	0	6	54	0	0
Vena cava stenosis	0	11	0	0	0	17	0	0	0	8	0	0	1	9	0	0	2	12	0	0	3	57	0	0
Coarctation of the aorta	3	8	0	0	3	14	0	0	4	4	0	0	1	9	0	0	0	14	0	0	11	49	0	0
Interrupted aortic arch	1	10	0	0	0	17	0	0	0	8	0	0	0	10	0	0	0	14	0	0	1	59	0	0
Major aortopulmonary collateral artery	0	11	0	0	0	17	0	0	0	8	0	0	0	10	0	0	1	13	0	0	1	59	0	0
Right aortic arch	2	9	0	0	1	16	0	0	0	8	0	0	0	10	0	0	0	14	0	0	3	57	0	0
Double superior vena cava (SVC)/left SVC	3	8	0	0	1	16	0	0	2	6	0	0	0	10	0	0	1	13	0	0	7	53	0	0
Coronary artery anomaly	1	10	0	0	0	17	0	0	2	5	0	1	4	6	0	0	1	13	0	0	8	51	0	1
Total	19	146	0	0	19	235	0	1	14	105	0	1	13	137	0	0	14	196	0	0	79	819	0	2

Accuracy: 99.8%.
TP, true positive; TN, true negative; FP, false positive; FN, false negative.

Table 5
Findings of other malformations at prospective ECG-triggering 320-row MDCT angiography in reference to surgical findings and/or conventional cardiac angiography.

	~1 month				1–3 months				4–6 months				6 months–1 year				1–2 years				Total			
Other malformations	TP	TN	FP	FN	TP	TN	FP	FN	TP	TN	FP	FN	TP	TN	FP	FN	TP	TN	FP	FN	TP	TN	FP	FN
Asplenia	3	8	0	0	0	17	0	0	0	8	0	0	0	10	0	0	0	14	0	0	3	57	0	0
Thymic hypoplasia	3	8	0	0	1	16	0	0	3	5	0	0	1	9	0	0	0	14	0	0	8	52	0	0
Tracheobronchial anomalies	2	9	0	0	2	15	0	0	0	8	0	0	0	10	0	0	0	14	0	0	4	56	0	0
Total	8	25	0	0	3	48	0	0	3	21	0	0	1	29	0	0	0	42	0	0	15	165	0	0

Accuracy: 100%.
TP, true positive; TN, true negative; FP, false positive; FN, false negative.

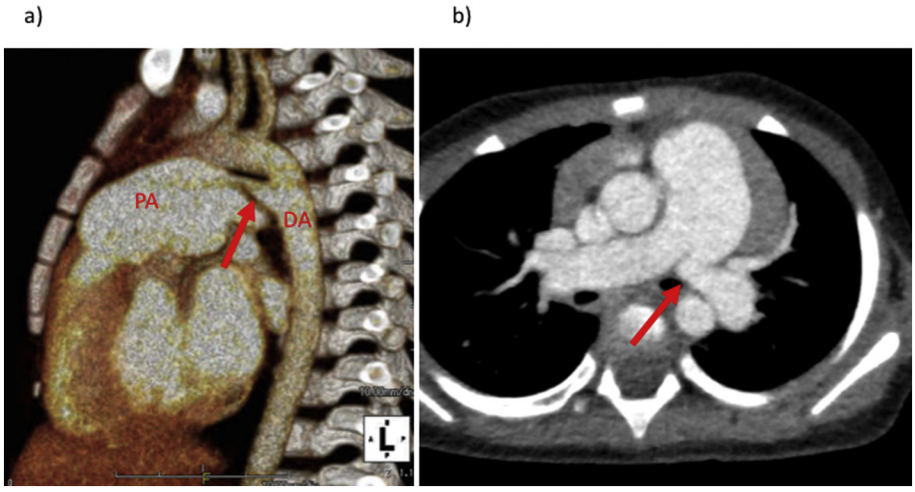

Fig. 1. A 1-year-old girl with a diagnosis of patent ductus arteriosus and left pulmonary artery stenosis. Prospective electrocardiogram-triggered 320-row computed tomographic angiography was performed at 80 kV and 55 mAs (effective dose, 0.97 mSv; heart rate, 120 beats/min). (a) Volume rendered image showing a patent ductus arteriosus (arrow). (b) Thick-section oblique-axial image showing a left pulmonary artery stenosis (arrow). PA, pulmonary artery; DA, descending aorta.

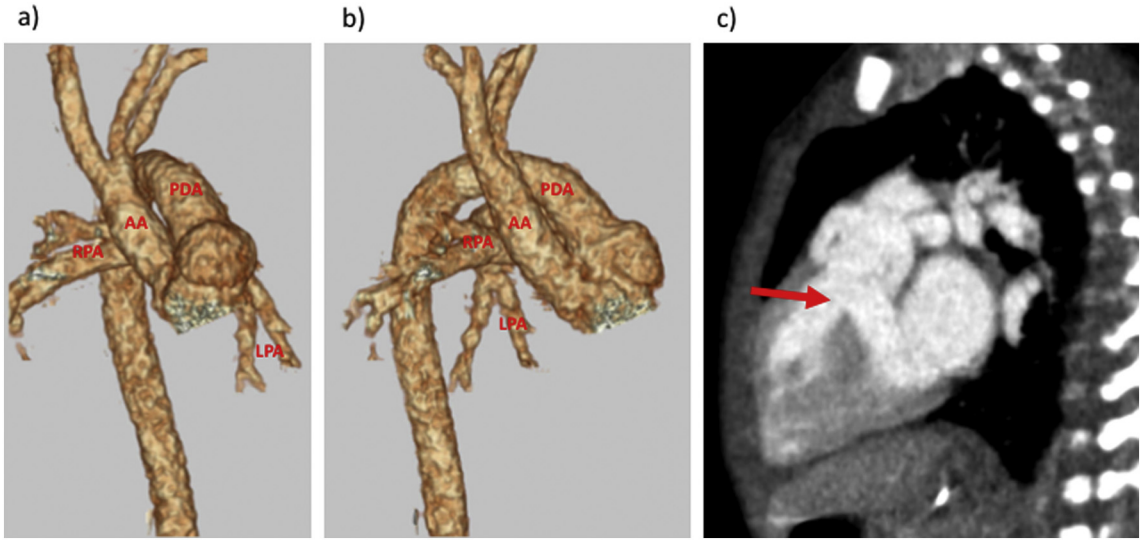

Fig. 2. A 4-day-old boy with a diagnosis of truncus arteriosus, an interrupted aortic arch, a patent ductus arteriosus, and a ventricular septal defect. Prospective electrocardiogram-triggered 320-row computed tomographic angiography was performed at 80 kV and 27 mAs (effective dose, 0.74 mSv; heart rate, 154 beats/min). (a, b) Volume rendered images clearly showing an interrupted aortic arch, bilateral pulmonary arteries arising from the ascending aorta, and a patent ductus arteriosus. (c) Thick-section oblique-sagittal image showing a ventricular septal defect (arrow). AA, ascending aorta; RPA, right pulmonary artery; LPA, left pulmonary artery.

assessment of complex CHD in infants; 2) the image quality score for each structure was diagnostic; and 3) intracardiac cardiovascular malformation before the age of 3 months or under a body weight of 5 kg and extracardiac cardiovascular malformation under the age of 6 months or under a body weight of 7.5 kg were occasionally missed.

Compared with transthoracic echocardiography, CT is more effective in demonstrating the extracardiac deformities present in complex CHD. It is very useful for demonstrating the anatomy of the pulmonary artery, along with the significant aortopulmonary collateral vessels. CT imaging also allows accurate identification of the aorta and pulmonary veins and their relationships. All pulmonary veins should be thoroughly investigated in a new patient with any type of CHD because an anomaly of these vessels could be the cause of unexplained severe pulmonary hypertension in pediatric patients. In echocardiography, turbulent flow on color Doppler should raise suspicion for pulmonary vein stenosis and monophasic flow, or flow velocities > 1.6 m/s indicate obstruction that may be functionally significant. However, evaluation of all pulmonary veins and accurate identification of the location of stenosis are sometimes difficult in young children even with a good acoustic window. CT angiography is an excellent technique for detailed analysis of the

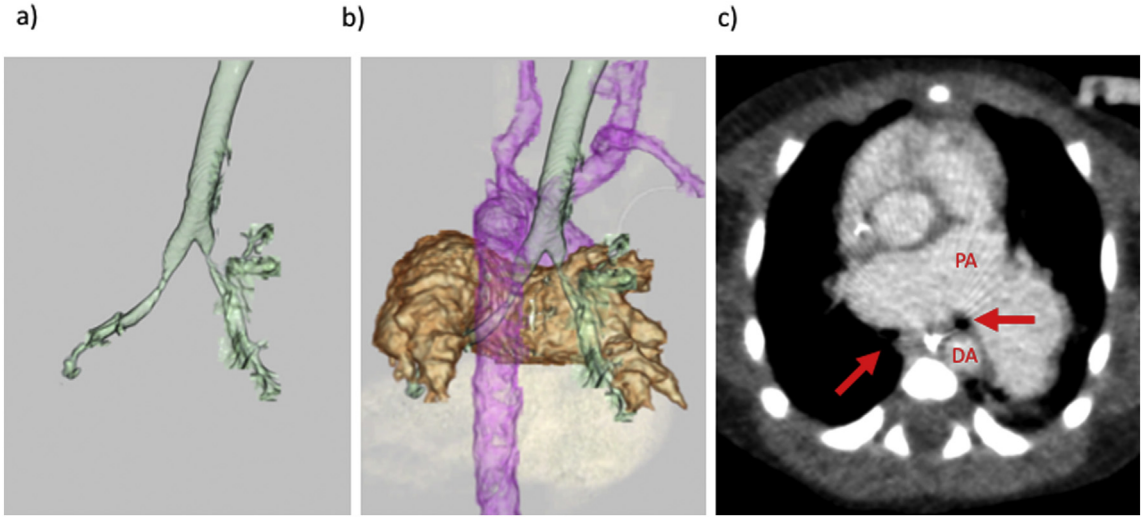

Fig. 3. A 2-day-old boy with a diagnosis of tetralogy of Fallot and absent pulmonary valve complicated by 22q.11.2 deletion. Prospective electrocardiogram-triggered 320-row computed tomographic angiography was performed at 80 kV and 34 mAs (effective dose, 1.08 mSv, heart rate: 116 beats/min). (a, b) Posterior view of volume rendered images showing the relationship of the bronchial tree (green), pulmonary artery (brown), and aortic arch (red). Volume rendered reconstruction images clearly depict a left bronchus that is compressed by a dilated pulmonary artery and descending aorta. (c) Thick-section oblique-axial image showing dilatation of the pulmonary artery, a bronchus that is compressed bilaterally (arrows), and a hypoplastic thymus. (For interpretation of the references to color in this figure legend, the reader is referred to the web version of this article.)

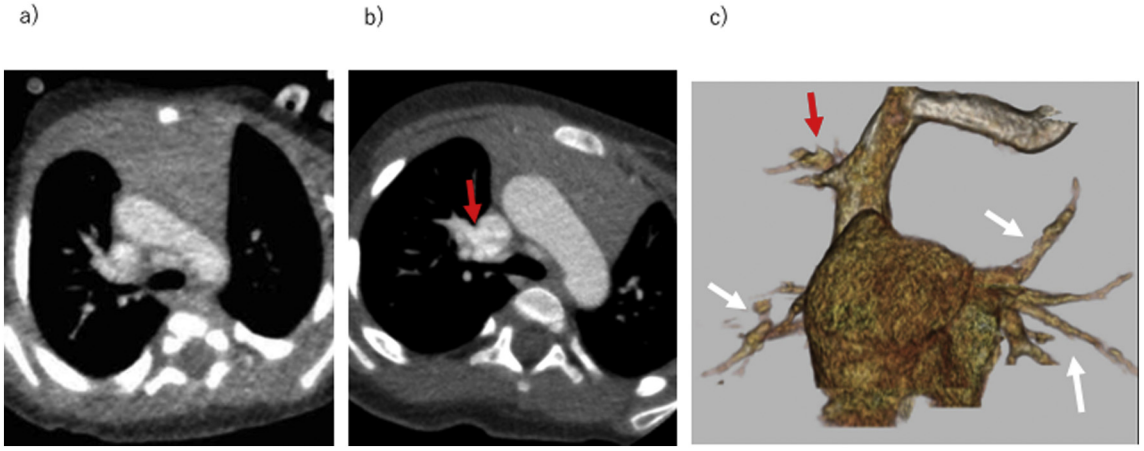

Fig. 4. A girl with a diagnosis of tetralogy of Fallot, patent ductus arteriosus, and partial anomalous pulmonary venous return at the age of 1 month (a) and 16 months (b, c). An anomalous connection of the right upper pulmonary vein to the superior vena cava is unclear at the age of 1 month but is clearly detectable at the age of 16 months.

pulmonary veins in patients with CHD. Therefore, our finding that all cases of pulmonary vein stenosis could be evaluated by 320-row CT is important (Fig. 5).

However, our study revealed that anomalous return of the right upper pulmonary vein in a small infant was difficult to diagnose (Fig. 4). A diagnosis of partial anomalous venous return should be made carefully because the venous wall between the pulmonary vein and superior vena cava may be too thin to be delineated on CT images, especially in a small infant.

A coronary artery anomaly was missed in a 4-month-old infant in this study. Coronary arteries are small structures and not easily assessed by CT in infants. The visibility of the coronary arteries in infants is influenced by several factors, including timing of breathing, heart rate, and body size. However, the diagnostic accuracy might be better in infants with a larger body size and a lower heart rate. Therefore, future studies focused on the diagnostic accuracy of coronary anomalies in larger patient populations are required.

There are several limitations to this study. First, we combined prospective ECG-triggered volume target scanning, a tube voltage setting of 80 kV, and an adapted hybrid iterative reconstruction technique to reduce the radiation dose without impairing image quality. However, the radiation exposure in our study was slightly greater than previously reported, [12,18] and might have been caused by wide craniocaudal-directional coverage. Patients with complex CHD are also likely to have other extracardiac malformations, like tracheal anomaly, which had a high prevalence in our study. Assessment of the bronchial tree, thymus, and isomerism are important for clinical management of complex CHD. In addition, the tube current was set by automatic exposure control and image noise was controlled at a low level (noise level, standard deviation 20; thickness, 0.5 mm) to maintain image quality for clinical use. This might have been the source of the excessive irradiation. Second, we excluded patients with valvular disease. We used a prospective ECG-gated scan, targeted only to the systolic phase to reduce radiation exposure. Therefore, evaluation of valvular disease would have been difficult using our protocol. However, assessment of valve morphology and motion is an important aspect of non-invasive echography and is not a problem in clinical practice. The clinical significance of CT is that it can substitute for invasive catheter

Table 6
Findings of all malformations at prospective ECG-triggering 320-row MDCT angiography in reference to surgical findings and/or conventional cardiac angiography based on patients' age.

	~1 month				1–3 months				4–6 months				6 months–1 year				1–2 years				Total			
	TP	TN	FP	FN	TP	TN	FP	FN	TP	TN	FP	FN	TP	TN	FP	FN	TP	TN	FP	FN	TP	TN	FP	FN
Intracardiac malformations	15	104	2	0	32	153	0	2	19	69	0	0	19	91	0	0	20	134	0	0	105	551	2	2
Extracardiac malformations	19	146	0	0	19	235	0	1	14	105	0	1	13	137	0	0	14	196	0	0	79	819	0	2
Other malformations	7	26	0	0	3	48	0	0	3	21	0	0	1	29	0	0	0	42	0	0	14	166	0	0
Total	41	277	2	0	54	436	0	3	34	197	0	1	32	258	0	0	33	373	0	0	193	1541	2	4

Accurate diagnosis of intracardiac malformation by 320-row CT: 3 month~.
Accurate diagnosis of extracardiac malformation by 320-row CT: 6 month~.
TP, true positive; TN, true negative; FP, false positive; FN, false negative.

Table 7
Findings of all malformations at prospective ECG-triggering 320-row MDCT angiography in reference to surgical findings and/or conventional cardiac angiography based on patients' body weight.

	~3 kg				3–5 kg				5–7.5 kg				7.5 kg–11 kg				Total			
	TP	TN	FP	FN	TP	TN	FP	FN	TP	TN	FP	FN	TP	TN	FP	FN	TP	TN	FP	FN
Intracardiac malformations	27	180	2	0	30	144	0	2	31	167	0	0	15	62	0	0	103	553	2	2
Extracardiac malformations	26	258	0	1	24	216	0	0	23	246	0	1	7	98	0	0	73	825	0	2
Other malformations	8	49	0	0	7	41	0	0	2	52	0	0	0	21	0	0	17	163	0	0
Total	60	488	2	1	60	402	0	2	51	470	0	1	22	181	0	0	193	1541	2	4

Accurate diagnosis of intracardiac malformation by 320-row CT: 5 kg.
Accurate diagnosis of extracardiac malformation by 320-row CT: 7.5 kg.
TP, true positive; TN, true negative; FP, false positive; FN, false negative.

Table 8
The image quality score at free-breathing prospective ECG-triggering 320-row MDCT angiography.

	~1 month	1–3 months	4–6 months	6 months–1 year	1–2 years	Total
Pulmonary artery	4.0 ± 0.0	4.0 ± 0.0	4.0 ± 0.0	4.1 ± 0.3	4.2 ± 0.4	4.1 ± 0.3
Pulmonary vein	3.9 ± 0.3	4.0 ± 0.0	4.0 ± 0.0	4.1 ± 0.3	4.2 ± 0.4	4.1 ± 0.3
Ascending aorta	4.0 ± 0.0	4.0 ± 0.0	4.0 ± 0.0	4.1 ± 0.3	4.2 ± 0.4	4.1 ± 0.3
Descending aorta	4.0 ± 0.0	4.0 ± 0.0	4.0 ± 0.0	4.1 ± 0.3	4.2 ± 0.4	4.1 ± 0.3
Superior vena cava	3.9 ± 0.2	3.9 ± 0.2	3.9 ± 0.2	4.1 ± 0.3	4.1 ± 0.6	4.0 ± 0.4
Inferior vena cava	3.6 ± 0.6	3.7 ± 0.4	3.8 ± 0.4	4.1 ± 0.4	4.0 ± 0.7	3.8 ± 0.5
Atrium	4.0 ± 0.0	4.0 ± 0.0	4.0 ± 0.0	4.1 ± 0.3	4.2 ± 0.4	4.1 ± 0.2
Ventricle	4.0 ± 0.0	4.0 ± 0.1	4.0 ± 0.0	4.1 ± 0.3	4.2 ± 0.4	4.1 ± 0.3
Bronchial tree	4.0 ± 0.0	4.0 ± 0.0	4.0 ± 0.0	4.1 ± 0.3	4.2 ± 0.4	4.1 ± 0.2
Overall quality	3.3 ± 0.3	3.4 ± 0.4	3.6 ± 0.2	3.9 ± 0.5	4.1 ± 0.6	3.7 ± 0.5

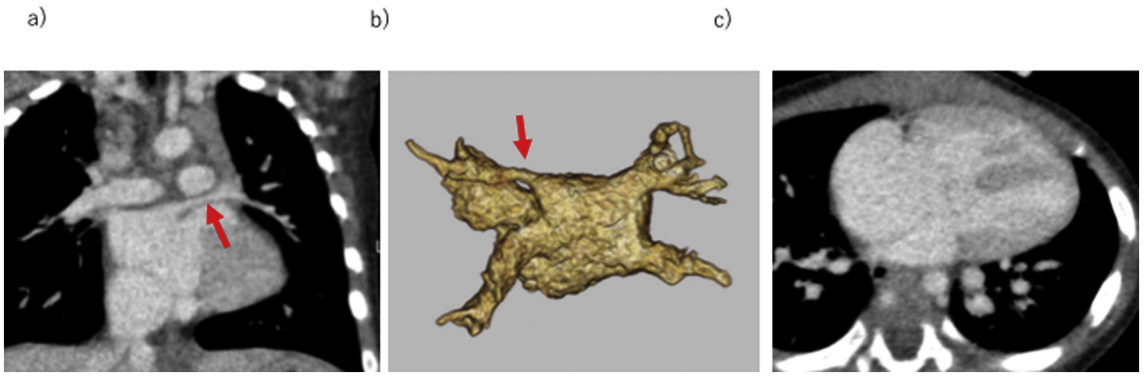

Fig. 5. An 8-month-old boy with a diagnosis of atrioventricular septal defect, left upper pulmonary vein stenosis complicated by Down syndrome. Prospective electrocardiogram-triggered 320-row computed tomographic angiography was performed at 80 kV and 45 mAs (effective dose, 1.15 mSv; heart rate, 133 beats/min). A thick-section coronal image (a) and a posterior view of a volume rendered image (b) clearly depict a left upper pulmonary vein stenosis. c) A thick-section oblique-axial image showing an atrioventricular septal defect.

angiography in patients with CHD.

In summary, second-generation 320-row CT angiography with prospective ECG-triggered volume target scanning and hybrid iterative reconstruction has high diagnostic accuracy in the assessment of complex CHD in infants. However, assessment of cardiovascular malformation is rather difficult in infants younger than 6 months or weighing < 7.5 kg, even with the latest 320-row CT scanner.

Funding sources

This work was supported by the Japan Society for the Promotion of Science (JSPS) KAKENHI (17K16452).

Acknowledgement

This work was supported by the Japan Society for the Promotion of Science (JSPS) KAKENHI (17K16452).

Conflict of interest

Y. Yamasaki: Bayer Healthcare Japan, Modest, Research Grant; Philips Electronics Japan, Modest, Research Grant.

Other authors: None.

References

[1] Vitiello R, McCrindle BW, Nykanen D, Freedom RM, Benson LN. Complications associated with pediatric cardiac catheterization. J Am Coll Cardiol 1998;32:1433–40.
[2] Bacher K, Bogaert E, Lapere R, De Wolf D, Thierens H. Patient-specific dose and radiation risk estimation in pediatric cardiac catheterization. Circulation 2005;111:83–9.
[3] Soongswang J, Nana A, Laohaprasitiporn D, et al. Limitation of transthoracic echocardiography in the diagnosis of congenital heart diseases. J Med Assoc Thai 2000;83(Suppl. 2):S111–7.
[4] Han BK, Overman DM, Grant K, et al. Non-sedated, free breathing cardiac CT for evaluation of complex congenital heart disease in neonates. J Cardiovasc Comput Tomogr 2013;7:354–60.
[5] Slovis TL. Sedation and anesthesia issues in pediatric imaging. Pediatr Radiol 2011;41(Suppl. 2):514–6.
[6] Dorfman AL, Odegard KC, Powell AJ, Laussen PC, Geva T. Risk factors for adverse events during cardiovascular magnetic resonance in congenital heart disease. J Cardiovasc Magn Reson 2007;9:793–8.
[7] Girshin M, Shapiro V, Rhee A, Ginsberg S, Inchiosa Jr. MA. Increased risk of general anesthesia for high-risk patients undergoing magnetic resonance imaging. J Comput Assist Tomogr 2009;33:312–5.
[8] Flick RP, Katusic SK, Colligan RC, et al. Cognitive and behavioral outcomes after early exposure to anesthesia and surgery. Pediatrics 2011;128:e1053–61.
[9] Wilder RT, Flick RP, Sprung J, et al. Early exposure to anesthesia and learning disabilities in a population-based birth cohort. Anesthesiology 2009;110:796–804.
[10] Ing C, DiMaggio C, Whitehouse A, et al. Long-term differences in language and cognitive function after childhood exposure to anesthesia. Pediatrics 2012;130:e476–85.
[11] DiMaggio C, Sun LS, Kakavouli A, Byrne MW, Li G. A retrospective cohort study of the association of anesthesia and hernia repair surgery with behavioral and developmental disorders in young children. J Neurosurg Anesthesiol 2009;21:286–91.
[12] Zhang T, Wang W, Luo Z, et al. Initial experience on the application of 320-row CT angiography with low-dose prospective ECG-triggered in children with congenital heart disease. Int J Cardiovasc Imaging 2012;28:1787–97.
[13] Nie P, Li H, Duan Y, et al. Impact of sinogram affirmed iterative reconstruction (SAFIRE) algorithm on image quality with 70 kVp-tube-voltage dual-source CT angiography in children with congenital heart disease. PLoS One 2014;9:e91123.
[14] < Appendix paediatric CT Dosimetry-2.pdf > .
[15] Ben Saad M, Rohnean A, Sigal-Cinqualbre A, Adler G, Paul JF. Evaluation of image quality and radiation dose of thoracic and coronary dual-source CT in 110 infants with congenital heart disease. Pediatr Radiol 2009;39:668–76.
[16] Stolzmann P, Scheffel H, Schertler T, et al. Radiation dose estimates in dual-source computed tomography coronary angiography. Eur Radiol 2008;18:592–9.
[17] Einstein AJ, Moser KW, Thompson RC, Cerqueira MD, Henzlova MJ. Radiation dose to patients from cardiac diagnostic imaging. Circulation 2007;116:1290–305.
[18] Cheng Z, Wang X, Duan Y, et al. Low-dose prospective ECG-triggering dual-source CT angiography in infants and children with complex congenital heart disease: first experience. Eur Radiol 2010;20:2503–11.